

A Feasibility Test for Indoor Magnetic Field Prediction

Seung-Sep Kim

Dept. of Geology and Earth
Environmental Sciences
Chungnam National University
Daejeon, South Korea
seungsep@cnu.kr

Sang-Mook Lee

School of Earth and Environmental
Sciences
Seoul National University
Seoul, South Korea
smlee@snu.ac.kr

Seong-Eun Kim, Eung Sun Kim

Samsung Advanced Institute of
Technology
Samsung Electronics
Yongin, South Korea
s.eun.kim,
eungsun.kim@samsung.com

Abstract—We examine feasibility for indoor magnetic field prediction based on generic information regarding building structure, which includes a floor plan and blueprint for determining quantities, sizes, shapes, and locations of reinforcing bars (or I-beams). Without measuring indoor magnetic field, such information may be sufficient to generate indoor magnetic map. We test this possibility by looking into two different types of construction: reinforcing-bar and I-beam building. A simple prism model is utilized to estimate magnetic field due to any given magnetic building material. The model, however, requires intensity and direction of magnetization for the given material, which limits the predictability of our approach. First, we assumed that the magnetization direction of building materials is uniform and parallel with the Earth field. Comparison between the predicted and measured magnetic fields for two buildings showed insignificant similarity, suggesting that the building materials would have their own direction of magnetization. This was confirmed by measuring magnetic fields over a rebar and two I-beams of 1-m length at magnetically quiet outdoor environment. The estimated intensities decrease with the total weight of the measured materials, while the estimated directions become more parallel with the Earth field. In order to examine a role of magnetization direction in indoor magnetic field, we divide the walls, floor, and ceiling of the measured space into numerous blocks and invert the measured data for the intensity and direction of magnetization of each block. The misfits between the modeled and observed magnetic field decrease faster by using more blocks for the walls than by using similar considerations for the floor and ceiling. The recovered direction of magnetization shows vertically oriented inclinations and randomly distributed declinations, which complicates prediction processes. Finally, we discuss the extent of predictability and ways to improve the modeling process.

Keywords—indoor magnetic map; magnetic field prediction; forward and inverse modeling

I. INTRODUCTION

Geomagnetic field varies in time and space because of internal structure of the Earth, external origins, and local magnetic perturbations [1]. While the two former contributors to the geomagnetic field are monitored at numerous magnetic

observatories, the local changes can be understood by well-planned magnetic surveys. Especially, the Earth's main field originated from internal sources and its secular variation are described by the International Geomagnetic Reference Field (IGRF) [2]. Using the IGRF model, one can find the direction and intensity of the Earth field at a given geographical location. Therefore, if magnetic materials are magnetized mainly in the direction of the Earth field, the magnetic perturbation resulting from the materials (e.g., man-made constructs) can be easily predicted with minimum usage of unknown parameters.

In this study, we examine feasibility for predicting indoor magnetic field based on generic information regarding building structure, obtainable from a floor plan and blueprint for determining quantities, sizes, shapes, and locations of reinforcing bars (or I-beams). If one can generate reliable indoor magnetic map without strenuously measuring indoor magnetic field, magnetic-based indoor navigation may become more practical and easy to be incorporated with other indoor navigation technologies [3].

II. MAGNETIC MODELING

We utilize a traditional geophysical method for estimating magnetic anomalies due to a 3-D arbitrary body with an arbitrary direction of magnetization [4]. A right-handed coordinate system is used with the axes x , y , z pointing toward geographical north, east, and downward, respectively. The magnetic field \mathbf{B} at any point $P(x, y, z)$ due to a body of volume V and magnetization \mathbf{m} located at (x_m, y_m, z_m) can be given by

$$\mathbf{B} = C_m \nabla^2 \int_V \mathbf{m}(r)^{-1} dV, \quad (1)$$

where $r = \sqrt{(x - x_m)^2 + (y - y_m)^2 + (z - z_m)^2}$ and $C_m = 10^{-7}$ for balancing units. By applying Laplace's equation and the Gauss divergence theorem, (1) can be converted into a set of surface integrals and simplified further into a set of analytic expressions for the given rectangular prism. For this study, the

analytic expressions are employed to calculate magnetic field due to magnetic materials for various magnetization directions and intensities [4, 5].

Estimation of the induced magnetic field \mathbf{B} requires knowing the volume of a magnetic body, its location, and direction and intensity (M) of magnetization. From the blue print of the building of interest, one can find the necessary information for volume and location of magnetic materials. Regarding magnetization of the materials, one needs to measure it directly in the lab or derive from the observed magnetic field. While changes in magnetization intensity modify amplitude of the magnetic field, changes in magnetization direction alter both amplitude and pattern of the field because the induced magnetic field is the net effect from the magnetized body in the direction of the inducing field. Thus, if the directions of magnetization and Earth field (i.e., inducing field) are sub-parallel, magnetic field prediction can become relatively simple for any given structure.

TABLE I. DIMENSIONS OF THE EXAMINED B MATERIALS

Type	Dimensions (mm)		Length (m)	Weight (kg)
RB1	Diameter	16	1	1.56
IB1	Beam height	200	1	50
	Flange ^a width	200		
	Web ^b thickness	8		
	Flange thickness	12		
IB2	Beam height	300	0.98	100
	Flange width	300		
	Web thickness	10		
	Flange thickness	14		

a. Flanges are the horizontal elements of 'I'.
b. Web is the vertical element of 'I'.

III. OUTDOOR MAGNETIC EXPERIMENTS

We chose two most commonly used building materials in South Korea to understand their magnetic properties. One is reinforcing bars for holding the concrete of the given structure in compression; another is I-beams for efficiently carrying both bending and shear loads from the structure. During the outdoor experiment, we measured magnetic fields over a reinforcing bar or rebar (RB1) and two I-beams (IB1 and IB2) using a three-component magnetometer at two different heights (0.8 and 1.2 m). The measurements were made along 10-m long north-south and east-west oriented survey lines, intersecting each other at the center of the survey space. First, a magnetic material was placed at the center parallel with one of the survey lines. Then, the measurements took place along both survey lines. The same measurement processes were repeated after relocating the magnetic material to become parallel with another survey line. In this way, we obtained both along- and across-profiles of magnetic field for each case. The measurements then were used to predict magnetic direction and intensity for the building materials. The declination and inclination of the Earth's magnetic field at the survey area given by the IGRF model are, $D_E = -7.6^\circ$ and $I_E = 51.6^\circ$, respectively. The main purpose of this outdoor experiment is to examine difference, if any, between directions of the Earth

field and magnetization of the given building materials. The physical dimensions of the magnetic materials are summarized in Table I.

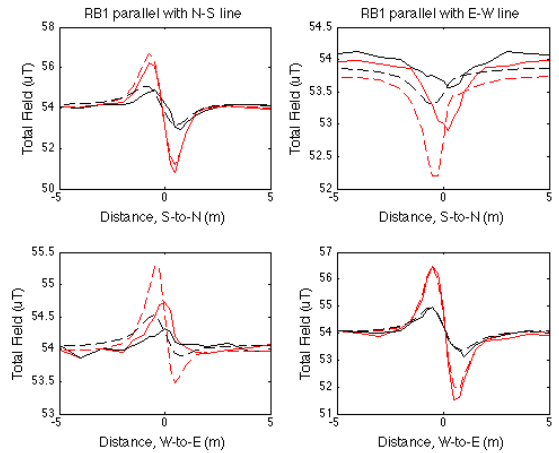


Figure 1. Comparison of the observed (solid line) and predicted (dashed) total magnetic field over RB1. The magnetic field observed at 0.8 m is in black and the observation made at 1.2 m is in red.

Using (1), we predicted magnetic due to the given magnetic materials and searched for the best model by minimizing rms misfits between the observed and predicted magnetic field. For RB1, the best model parameters are $M_{RB1} = 97,000$ A/m, $D_{RB1} = -13^\circ$, and $I_{RB1} = 9^\circ$ (Fig.1). Similarly, we find the best model parameters for IB1 (Fig. 2) as $M_{IB1} = 4,400$ A/m, $D_{IB1} = -8^\circ$, and $I_{IB1} = 2^\circ$ and for IB2 (Fig. 3) as $M_{IB2} = 400$ A/m, $D_{IB2} = -7^\circ$, and $I_{IB2} = 36^\circ$.

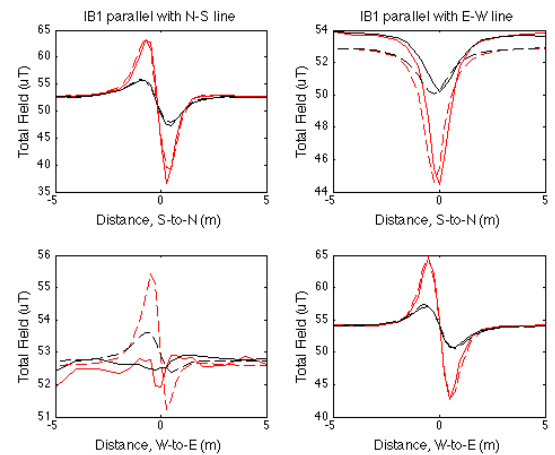


Figure 2. Comparison of the observed (solid line) and predicted (dashed) total magnetic field over IB1.

The predicted parameters describing magnetization of the tested building materials are rather striking because the magnetization intensity for RB1 (thinnest and lightest) is 20 or 200 times higher than the examined I-beams. Such significant contrast may be understood in terms of differences between

manufacturing processes of rebar and I-beam. Apart from the detailed mechanical processes, the main factor related with magnetization is the cooling time after heating steel scraps generally above the Curie temperature, where previous magnetic properties are completely erased [4]. As the given magnetic material cools below the Curie temperature, the spinning electrons in atoms become aligned in the direction of inducing magnetic field (presumably Earth field). At the same time, a magnetic domain is formed by these aligned spins. If a magnetic material were of only one magnetic domain, it would have a strong magnetic field. To reduce the magnetostatic energy, however, the material generally is split into many domains pointing in different directions. In addition, for multi-domain magnetic materials, slower cooling allows more time to acquire lower magnetization due to self-demagnetization [6]. Hence, the faster cooling for increasing mechanical strength of rebar appears to be effective to achieve higher magnetization because RB1 has less time to generate sufficient number of magnetic domains to decrease the stored energy and to be subjected to self-demagnetization.

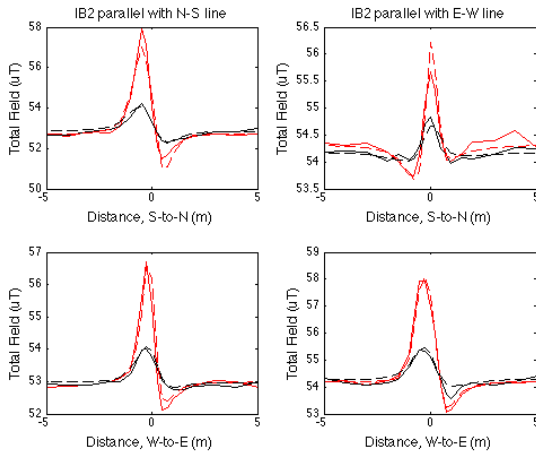


Figure 3. Comparison of the observed (solid line) and predicted (dashed) total magnetic field over IB2.

Interestingly, as the estimated magnetization intensity decreases, the predicted magnetization direction becomes closer to the direction of the Earth field. For the given cooling time, the magnetic materials may obtain different degree of the net alignment of magnetic domains. For example, IB2 has longer cooling time, as thicker slab requires more time to be quenched, and hence can produce more magnetic domains. Because the directions of the magnetic domains are aligned to reduce magnetostatic energy, the net direction of the magnetic domains becomes random. As a result, IB2 does not acquire a unique direction of magnetization. The induced magnetic field of IB2 can be predicted using the direction of the inducing field (the Earth field for our case). RB1 and IB1, however, appear to have their own directions of magnetization that modulate amplitude and shape of induced magnetic field. Thus, the estimation of magnetic field for a building composed of RB1 or IB1 can be computationally expensive because the net effect of magnetization directions of individual material pointing in different directions needs to be calculated.

IV. INDOOR MAGNETIC EXPERIMENTS

We have measured indoor magnetic field from two different constructs: one is built with reinforcing bars and another with I-beams. Measurement spacing was 20 cm and sensor heights varied from 0.8 m to 1.6 m with 0.2 m step. A non-magnetic moving platform was used to locate the sensor precisely on the pre-designed measurement points and move it to the next point faster. The total field was calculated from the measured three-component magnetic fields at each height and then inverted for direction and intensity of magnetization for a given set of rectangular prisms, which approximates the indoor constructional environments (e.g., walls, floor, and ceiling). Because the net sum of individual magnetic materials pointing in different directions is problematic, we assume that the net result can be approximated by the magnetization of a rectangular prism (i.e., the subdivision of the indoor building construct). The best model parameters minimizing the chi-square misfit between prediction and observation were estimated using the Levenberg-Marquardt method [7].

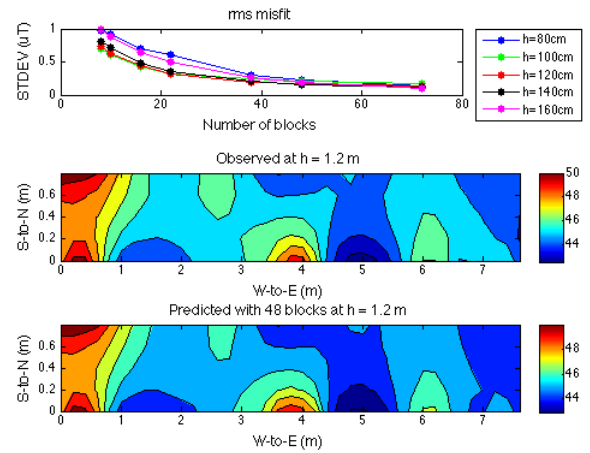


Figure 4. As the number of blocks increases, rms misfits between the observed and predicted data decrease rapidly (top panel) for the reinforcing-bar building. Comparison of the observed (middle panel) and predicted (bottom panel) data using 48 block model illustrates the goodness of fit.

The measurement space of the reinforcing-bar building is the hallway of the first floor bounded by two east-west trending walls. These walls are discontinued by the doors to individual rooms. The western and eastern ends of this space are open because we limited our survey within the central part of the hallway. We assume the observed indoor magnetic field is mainly due to the net result of reinforcing bars installed into floor, ceiling, and walls. In Fig. 4, the standard deviation of rms misfits between the model and data (top panel) decreases as more blocks are used to approximate the given hallway structure. The first rapid decrease in the misfits occurs when the walls are divided only and both floor and ceiling are kept as one block for each. It indicates that the observed spatial variation of indoor magnetic field is mainly governed by how walls are divided (middle panel). The later refinement results from the division of floor and ceiling. In addition, the misfits for the middle range of the measurement heights are smaller than the lowest (closest to floor) and highest (closest to

ceiling) sensor heights. Such variation implies that the observed fields at these heights contain more effects from constituents (e.g., pipes and electric wires) installed into floor and ceiling than the walls, which are not incorporated into our model.

For the I-beam building, the measurement space is the hallway of the second floor bounded by two steal doors at the eastern end and the center of the northern boundary, and 1-m tall walls made of steal plates. The northern boundary is the most complicated structure because of the door leading to the stairs, an electrical enclosure, and a housing for various pipes. We also assume that the net effect of these components and I-beams can be approximated by the magnetization of prism blocks. Similar to the rebar building, the consideration on the walls of the I-beam building appears to be more effective to decrease overall misfits between the model and data (Fig. 5). The misfit at the lowest sensor height decreases slower than other heights. The ceiling height of the building is about 3.2 m so the measurements at 1.6 m are still far away from magnetic effects due to other installed parts at ceiling.

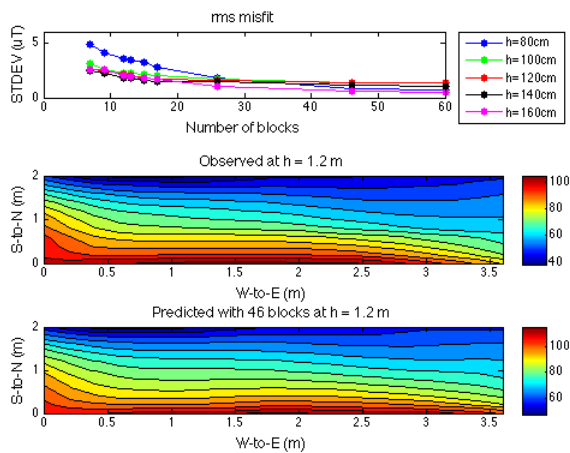


Figure 5. As the number of blocks increases, rms misfits between the observed and predicted data decrease rapidly (top panel) for the I-beam building. Comparison of the observed (middle panel) and predicted (bottom panel) data using 46 block model illustrates the goodness of fit.

The major difference between the observed data from the rebar and I-beam building is the range of the magnitude of the total magnetic field. The magnitude of I-beam building's indoor magnetic field is about twice larger than that of rebar building (Figs. 4 and 5). From the outdoor experiment, we found that the magnetization intensity of rebar is larger than that of I-beam. However, the magnetization direction of I-beam is similar to the Earth field's direction. The indoor magnetic field of the rebar building reflects the net effect of difference between reinforcing bars pointing in different directions and between the Earth field and magnetization direction of rebar. Contrary to the rebar building, the indoor field of the I-beam building has less chance to experience such canceling-out effect caused by differences in magnetization direction. Instead, the summing effects between magnetic fields induced from

nearby I-beams appear to be more prominent. Thus, we observe the reduced indoor magnetic field from the rebar building consisted of the materials having high magnetization intensity and exceptionally strong indoor field from the I-beam building composed of the I-beams characterized with low magnetization intensity.

V. DISCUSSION

Both outdoor and indoor experiments stress the importance of magnetization direction in predicting indoor magnetic field for a given building. If the magnetization direction of the main building material is sub-parallel with the inducing field, estimating the resulting induced magnetic field can be relatively simple because magnetization intensity does not change the shape of the magnetic field. In addition, such case reduces cancelling effects due to the magnetization vector pointing in different directions. For this case, thus, few observations are required to construct indoor magnetic map. In this respect, the feasibility of indoor magnetic field prediction for I-beam buildings is slightly better than that for rebar buildings, although smoothly varying magnetic field of the I-beam building (Fig. 5) may not be ideal for indoor navigation.

To improve feasibility of indoor magnetic field prediction, one can build a stochastic study to approximate the net effect of magnetic materials pointing in different directions and having different magnetization intensity. In addition, a database for magnetic properties of building materials can be useful to enhance the reliability of the model.

ACKNOWLEDGMENT

We thank the students from Yeungnam University for making systematic magnetic field measurements in outdoor and indoor environments. This study was supported by Samsung Electronics.

REFERENCES

- [1] W. M. Telford, L. P. Geldart, R. E. Sheriff, and D. A. Keys, *Applied Geophysics*. London: Cambridge Univ. Press, 1986.
- [2] C. C. Finlay, S. Maus, C. D. Beggan, T. N. Bondar, A. Chambodut, T. A. Chernova, A. Chulliat, V. P. Golovkov, B. Hamilton, M. Hamoudi, R. Holme, G. Hulot, W. Kuang, B. Langlais, V. Lesur, F. J. Lowes, H. Lühr, S. Macmillan, M. Manda, S. McLean, C. Manoj, M. Menvielle, I. Michaelis, N. Olsen, J. Rauberg, M. Rother, T. J. Sabaka, A. Tangborn, L. Toffner-Clausen, E. Thébault, A. W. P. Thomson, I. Wardinski, Z. Wei, and T. I. Zvereva, "International Geomagnetic Reference Field: the eleventh generation," *Geophys. J. Int.*, vol. 183, pp. 1216-1230, 2010.
- [3] R. Mautz, "Overview of indoor positioning technologies," *IPIN*, Keynote presentation, 2011.
- [4] P. V. Sharma, *Geophysical Methods in Geology* vol. 2nd. New York: Elsevier, 1986.
- [5] A. Pignatelli, I. Nicolosi, R. Carluccio, M. Chiappini, and R. von Frese, "Graphical interactive generation of gravity and magnetic fields," *Computers & Geosciences*, vol. 37, pp. 567-572, 2011.
- [6] Y. Yu, "Importance of cooling rate dependence of thermoremanence in paleointensity determination," *J. Geophys. Res.*, vol. 116, p. B09101, 2011.
- [7] W. H. Press, S. A. Teukolsky, W. T. Vetterling, and B. P. Flannery, *Numerical recipes in C: the art of scientific computing*, 2nd ed. London: Cambridge Univ. Press, 1992.